Engineering Fracture Mechanics 310 (2024) 110421

Contents lists available at ScienceDirect

Engineering Fracture Mechanics

journal homepage: www.elsevier.com/locate/engfracmech

The damage Mechanics challenge Results: Participant predictions compared with experiment

J.P. Morris [a,*], L.J. Pyrak-Nolte [b], H. Yoon [c], A. Bobet [b], L. Jiang [b,d]

[a] Lawrence Livermore National Laboratory, Livermore, CA, USA
[b] Purdue University, West Lafayette, IN, USA
[c] Sandia National Laboratories, Albuquerque, NM, USA
[d] Now at: State Key Laboratory of Hydroscience and Engineering, Tsinghua University, Beijing, China

ABSTRACT

We present results from a recent exercise where participating organizations were asked to provide model-based blind predictions of damage evolution in 3D-printed geomaterial analogue test articles. Participants were provided with a range of data characterizing both the undamaged state (e.g., ultrasonic measurements) and damage evolution (e.g., 3-point bending, unconfined compression, and Brazilian testing) of the material. In this paper, we focus on comparisons between the participants' predictions and the previously secret challenge problem experimental observations. We present valuable lessons learned for the application of numerical methods to deformation and failure in brittle-ductile materials. The exercise also enables us to identify which specific types of calibration data were of most utility to the participants in developing their predictions. Further, we identify additional data that would have been useful for participants to improve the confidence of their predictions. Consequently, this work improves our understanding of how to better characterize a material to enable more accurate prediction of damage and failure propagation in natural and engineered brittle-ductile materials.

1. Introduction

Understanding the failure of materials is particularly relevant today with the current interest in aging infrastructure and in enhanced geothermal systems which require a network of fractures to optimize production. As more and more sensors are used to monitor infrastructure and the subsurface, methods are required to detect anomalous signals in data and link these signals to the underlying physics and mechanics of failure to determine if failure is imminent. This requires robust computational methods that capture the physics of failure and identify the measurable signatures of failures. While there are many computational approaches for simulating damage evolution in materials, few have been ground-truth tested with either known experimental data or with blind data sets.

The Fracture Challenge concept (e.g., [2]) has demonstrated that valuable lessons can be learned by comparing computational methods and workflow approaches taken by different teams in the blind prediction of controlled fracturing experiments. Previous challenges have focused upon failure in metals. Here, we present results from a challenge that considered damage evolution in additively manufactured samples where the mechanical response is similar to the brittle-ductile response of many rocks, yet highly reproducible from one test article to another by virtue of the 3D printing process.

The experimental design was developed as a community effort at a Damage Mechanics Workshop held at Purdue University in February 2019 which included leading computational scientists and engineers in the field of computational damage mechanics. The goals of the challenge were to:

* Corresponding author.
E-mail address: morris50@llnl.gov (J.P. Morris).

https://doi.org/10.1016/j.engfracmech.2024.110421
Received 4 January 2024; Received in revised form 12 July 2024; Accepted 20 August 2024
Available online 22 August 2024
0013-7944/Published by Elsevier Ltd.

1. Compare computational approaches for damage evolution for predicting fracture behavior of 3D printed model rock;
2. Identify the information provided by the different simulation approaches that gives insight into the prediction and interpretation of failure in rock;
3. Identify model parameters that are currently not measured or cannot be measured in the laboratory; and
4. Determine whether there are other experimental measurements that are needed or better methods of performing measurements to monitor damage evolution.

The challenge provided insight into the state of the art and future directions to improve the community's ability to simulate crack formation and evolution in natural and engineered brittle-ductile materials. The benchmark dataset is available for others in the community to test their computational approaches [7,8] and for training graduate and undergraduate students in methods for verification of computational models with experimental data.

2. The challenge process

The challenge focused on the prediction of brittle-ductile failure of a notched test specimen (Fig. 1, left) under 3-point bending loading conditions. All specimens were created using a 3D printing process (Projet CJP 360) where layers of calcium sulfate hemihydrate were deposited and then bonded with a manufacturer's proprietary water-based binder that produces gypsum as a reaction product. The gypsum mineral growth direction is influenced by the direction in which the binder is sprayed and results in an oriented mineral fabric[6](Fig. 1, right). Full details of the data provided for calibration, along with the challenge problem, are provided in the companion paper, Jiang et al. (in review) in this special issue. Participants were provided with a range of data that characterized:

1. the undamaged state:
   a. ultrasonic measurements
2. damage evolution
   a. 3-point bending for a range of notched calibration geometries (see Fig. 2)
   b. unconfined compression
   c. Brazilian testing

Participants were then required to perform a blind prediction of the progressive failure of a notched specimen under 3-point bending of a unique notch geometry that was not part of the calibration data set. There was a period of over a year between the publishing of the calibration data with the challenge problem description and the due date for participants to provide their predictions of the behavior of the challenge geometry. During this period, participants were encouraged to collaborate, and a workshop was held to enable comparisons of approaches to model calibration (see Section 5). We refer to the initial phase of model calibration as the "Calibration Phase" (CA for short) and the subsequent focus upon the blind predictions as the "Challenge Phase" (CH for short). We designate the workshop held in June 2022 as the end of the calibration phase and beginning of the challenge phase.

3. The teams and numerical methods

Teams responded to both the calibration (CA) and challenge (CH) phases and employed a range of numerical methods. We define calibration phase participants as those who submitted calibration results in time for the June 2022 workshop. Table 1 lists the teams, their methods, and their participation in the phases. We observe that two teams that participated in the calibration phase did not ultimately submit predictions for the challenge problem, and that one additional team joined only after the workshop.

The range of computational methods employed allows us to explore some of the respective advantages associated with each of the

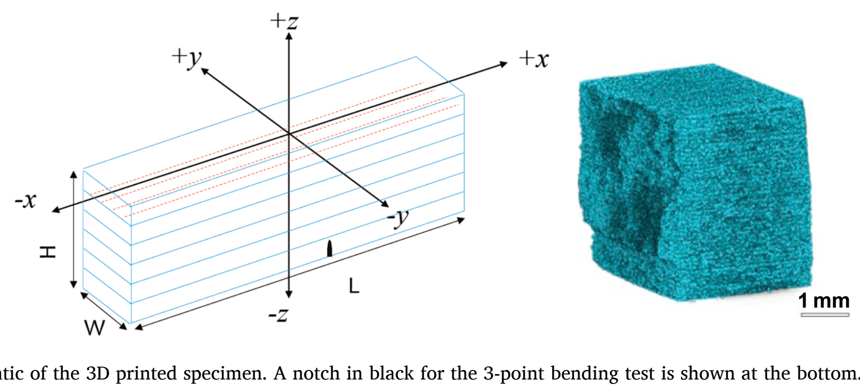

Fig. 1. Left: A schematic of the 3D printed specimen. A notch in black for the 3-point bending test is shown at the bottom. Red lines indicate the binder spreading direction. Blue lines are the depositional layer orientation. Each layer is approximately 100 μm (Line separations are not drawn to scale). W=12.7 mm, L=76.2 mm, and H=25.4 mm. Right: X-ray tomographic reconstruction of 3D printed gypsum sample showing bedding/layering and fabric structure (Jiang et al. (in review)).

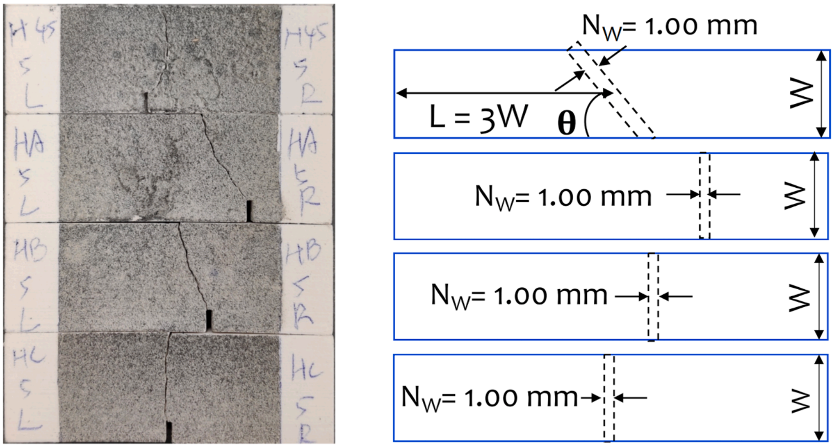

Fig. 2. The calibration test specimens had a range of notch locations and orientations to induce different failure modes. However, all calibration notches had the same notch depth. Side view of failed test articles (left) and top-down view of schematics (right).

techniques. Previous papers have provided detailed reviews of numerical methods for discontinuities in rock mechanics[9,1,5]. In addition, companion papers in this issue provide more specific explanations of the methods utilized by the challengers [19–23]. Here we provide a high-level description of the methods and some general comments regarding their advantages:

- Particle Flow Codes / Bonded Particle Methods generally treat the intact medium as a collection of circular (2D) or spherical (3D) particles that have inter-particle forces intended to mimic the elastic–plastic response of the rock. Such methods are algorithmically very simple and intuitive, and yet can reproduce realistic rock-like behavior. One challenge for such approaches is that the bond constitutive response (both elastic and failure) must be tuned to match the upscaled rock response (e.g. [17]). In addition, these methods usually require that cracks propagate along existing particle–particle boundaries, causing the initial particle arrangement to influence the crack propagation.
- The Finite/Discrete Element Method (FDEM) treats intact material deformation with finite elements[9] and allows for the elements to become separated to accommodate evolution of cracks along the faces of the finite elements. Being built on finite elements, such methods have a rigorous approach to accommodate elastic moduli and complex constitutive laws. In the simplest implementations, stiff cohesive elements are introduced at face boundaries upon model initialization and are allowed to subsequently fail (Ortiz and Pandolfi [12]). Such an approach is algorithmically simple but can lead to a very stiff system of discrete equations to solve. FDEM can also be implemented such that cohesive elements are introduced dynamically as finite element interfaces fail[10,3]. While more algorithmically complex, such approaches avoid the additional compliance introduced by cohesive elements being present upon initialization. The attraction of FDEM is that it is generally algorithmically simple, runs fast, and can be readily coupled with other physics, such as fluid flow between elements[14]. Most implementations of FDEM require that the evolving cracks follow the faces of the initial mesh. This can result in crack propagation that shows mesh imprinting. This effect can be reduced somewhat by utilizing tetrahedral meshes that are intentionally disordered to increase the likelihood of element faces aligned with the preferred crack direction[15,16]. Mesh imprinting can be reduced further by remeshing to accommodate the preferred crack direction (for example, [11]), but the algorithmic complexity associated with this approach, and the additional challenges of coupling it to other methods, makes this less commonly utilized.
- Hybrid Discontinuous Galerkin (HDG) methods are related to Discontinuous Galerkin (DG) methods (see Radovitzky et al. [13]). Compared with traditional FEM, DG methods have better treatments for higher order operators, support simple and unambiguous enforcement of boundary conditions (such as on a crack face), and perform better than traditional FEM on arbitrary meshes. DG methods introduce a large number of additional degrees of freedom (DoF), and the HDG approach significantly reduces this by only

Table 1
List of teams, numerical methods, and involvement in the calibration (CA) and challenge (CH) phases of the exercise.

Team	Methods	Participation
FDEM team Toronto	Finite/Discrete Element Method (FDEM)	CA/—
GRIPHFITH	Phase Field	CA/CH
Imperial-Vanderbilt-Oviedo	Phase Field	CA/CH
Lion Rock	FDEM	CA/—
MIT TU Delft	Hybrid Discontinuous Galerkin Model	CA/CH
Montana Tech Team	PFC3D / FDEM	CA/—
LANL	FDEM	––/CH

selectively introducing DoFs. Like FDEM approaches, HDG will show mesh imprinting on the crack trajectory unless remeshing in the crack tip zone is employed.

- The Phase Field Method (PFM) is an example of a continuous approach to fracture. Unlike the methods described previously, PFM does not introduce discontinuities into the displacement field. PFM introduces an intrinsic length scale and smears cracks over a localization band of finite width. The crack is diffusely represented by a (phase) field variable, and equations are introduced to control the evolution of the phase field so as to accommodate crack propagation. Most implementations of PFM utilize FEM to solve the governing equations. However, some authors have utilized other discretizations to better treat the high-order phase field equations. Zhuang et al. [18] provide a recent review of PFM with a focus on different implementation approaches. Because cracks are tracked implicitly via the phase field, the evolution of the crack geometry is less sensitive than what is observed for FDEM methods. PFM simulations typically require very high resolution, leading to high computational expense. However, adaptive mesh refinement can alleviate this limitation to some degree (see [4]). In addition, coupling of PFM with other physical processes, such as fluid flow on fractures, has proven more challenging than for FDEM.

4. Approach to error metrics

As demonstrated by the companion paper describing the calibration and challenge data, the experimental results were very repeatable, with some variation among the test specimens of a given geometry. Consequently, it was determined that the error estimate should be based upon the difference between the simulation prediction and the envelope of the experimental results. In addition, it was necessary to extrapolate the predictions in many cases before comparing with data. This is essential; otherwise, a simulation result corresponding to a single point would have zero error if it happened to fall within the band of the experimental results. For force–displacement predictions, a force of zero was assumed if a simulation provided no estimate. For crack propagation, if a predicted crack did not propagate to the edge of the test specimen, it was assumed that it propagated directly to the closest surface.

To provide some sense of relative error, the extrema of the average of the experimental results were calculated and used to construct a reference area in solution space. Subsequent sections will present calculations of the area of discrepancy between the predictions and the envelope of the experiments and compare this with the reference area to obtain a percentage error. Fig. 3 and Fig. 4 plot these reference area rectangles for the force–displacement and crack geometries, respectively.

A second approach for error calculation was based upon what fraction of the crack length is outside of the envelope of the experimental results. We shift the simulated cracks in the x-direction, seeking the shift with minimum discrepancy in order to allow for the possibility that the point of initiation may differ, but the crack geometry otherwise be consistent with experiment. In this approach, the error was the total of the portion of the simulated crack that either fell outside the envelop of the experimental results or where no simulated crack was reported because the simulated crack did not reach the edge of the specimen (see Fig. 5). With this error measure, a perfect score would have an error of 0% and shift of 0 mm.

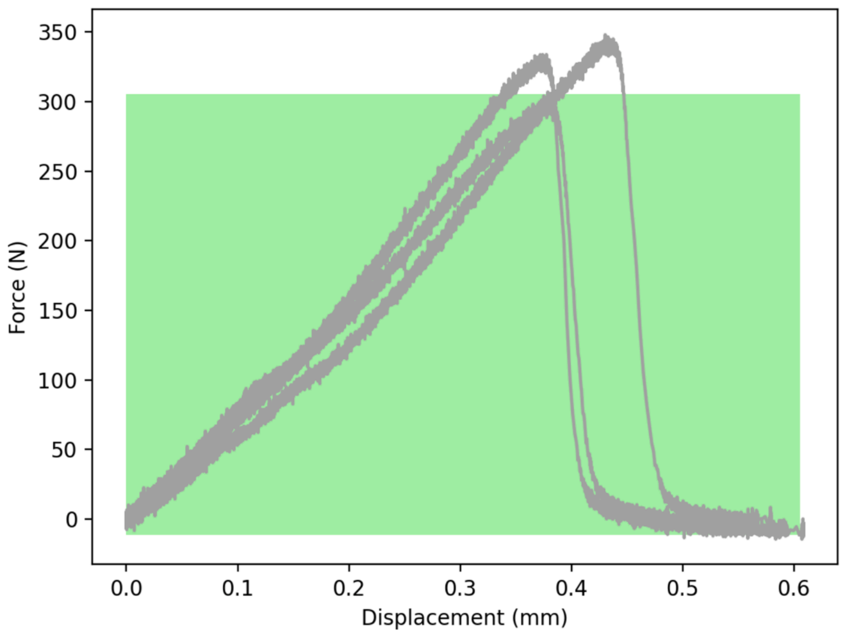

Fig. 3. The force–displacement data for the challenge geometry, shown with a representative area that bounds the extrema of the average response.

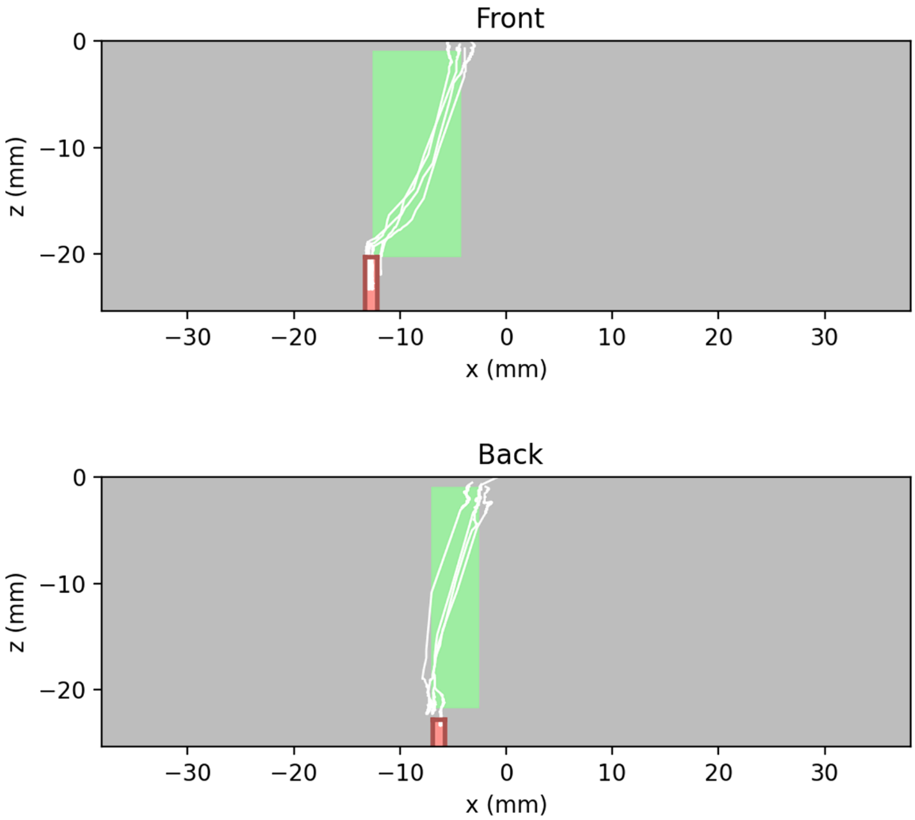

Fig. 4. Experimentally observed crack trajectories for the front and back of the test articles. The cracks are plotted in white, with the green rectangles corresponding to the bounding box of the average crack trajectories.

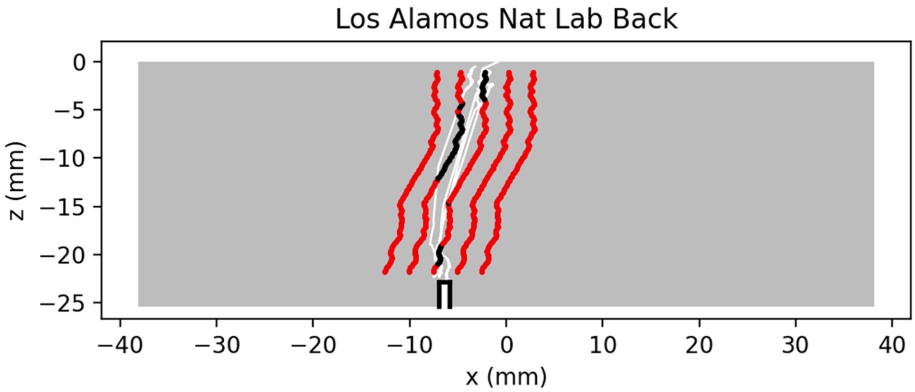

Fig. 5. A linear-based approach to error estimation was based upon the fraction of the crack that is outside (shown in red) of the envelope of the experimental results. We shift the simulated cracks in the *x*-direction, seeking the minimum discrepancies in order to allow for the possibility that the point of initiation may differ, but the crack geometry otherwise be consistent with experiment.

5. The calibration phase

All participants were invited to participate collaboratively on a voluntary basis while calibrating their models. This period culminated in a special workshop entitled "*Damage Mechanics Challenge Workshop*" held at the 56th US Rock Mechanics/Geomechanics Symposium on *June 25th, 2022*. This workshop provided an opportunity for participants to compare calibration procedures and calibration performance for the calibration notch geometries (Fig. 2), but discussion of results for the challenge geometry was prohibited. This exercise was an important step to ensure that participants had a chance to learn as much as possible from the calibration data and avoid needless pitfalls as they approached the challenge phase. A representative subset of the results revealed at the workshop

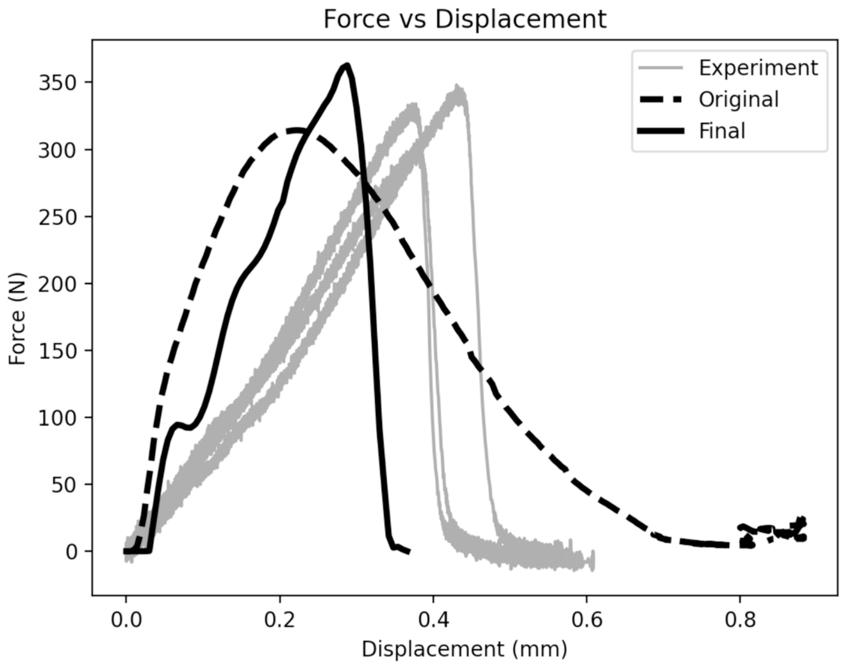

Fig. 6. An example of an initially poor calibration result for the force–displacement response of the central-notched specimens as obtained by the FDEM team Toronto. The team decided to calibrate elastic parameters to the ultrasonic data, resulting in an excessively stiff initial response. Later, the team performed a separate calibration ignoring the ultrasonic data, achieving an improved fit to the data (solid line), although still not as good as some other teams (see Fig. 7) at this point in the Challenge.

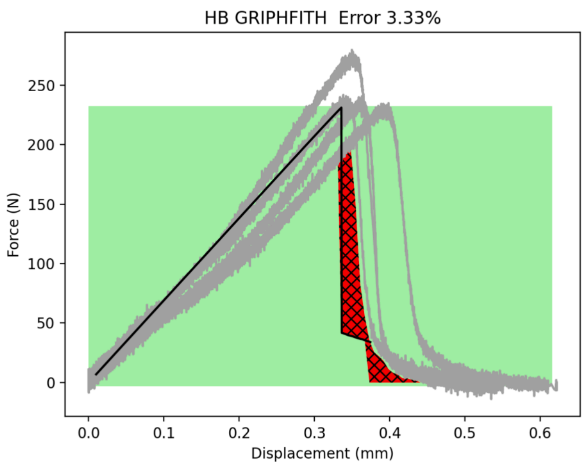

Fig. 7. An example of a more successful calibration result for the force–displacement response of the central-notched specimens. Here the team decided to ignore using the ultrasonic moduli and focused upon calibration against the stress–strain response to obtain the initial elastic loading response. Here the error (red cross-hatched area divided into the green area) is 3.33%.

is shown in Fig. 6 and Fig. 7. Of particular interest is that participants' predictions fell into one of two groups:

1. errors in load–displacement were greater than 30% (Fig. 6).
2. errors in calibration to load displacement were only a few percent (Fig. 7)

Discussion of the results and calibration procedures during the calibration workshop revealed that:

- The largest deviations from experiment were from teams that calibrated with ultrasonic, UCS, and Brazilian tests and performed blind predictions of 3-point bending tests.

- The best calibration results were achieved by including the 3-point bending data for calibration of both the elastic and damage model parameters.

A factor contributing to the large discrepancies was that the observed stiffness of the test articles inferred by ultrasonic measurement was significantly greater than that implied by the 3-point bending tests. Possible explanations are:

- The stress state during 3-point bending is more tensile than during the ultrasonic tests, leading to opening of microcracks and a reduction in modulus.
- The moduli are rate dependent and the lower-rate 3-point bending test experiences a lower apparent modulus than the dynamic ultrasonic measurement.

In general, moduli determined from static methods are usually lower than those determined from ultrasonic methods. Once the teams realized the relative value of the different data for the purpose of calibration, they were all able to subsequently achieve a similar agreement to the calibration of 3-point bending tests. Consequently, it was concluded that collaboration during the calibration phase was essential for enabling teams to fairly compete for the challenge problem.

6. The challenge phase

The challenge geometry included an offset angled, non-uniform depth notch, intended to induce Modes I, II, and III (see Fig. 8). This notch geometry was intended to exercise slightly different combinations of failure mode during the failure of the test specimen. As such, the expectation was that it would prove more challenging than the calibration geometries.

Challengers were asked to provide responses to several questions. Each question typically involved quantitative reporting of the results of their predictions with the intention of direct comparison against the experimental results. Here we report the questions, along with general comments about the level of participation and the utility of the results reported.

Challenge Question 1: Report the best prediction of force–displacement curve from initial loading through post-peak failure. The displacement value should be the vertical (z) displacement at the contact point with the central rod. Label each load with a point number to enable linking the data reported for Question 1 to results reported for questions 2 & 3.

- All challengers reported results for this question. This data proved to be readily appropriate for direct, quantifiable comparison with the experimental results.

Challenge Question 2: Report a series of x, y, z points that define a line representing the position of the crack tip from the notch as a function of load and displacement from initial loading through post-peak. If there are multiple cracks, report the information for each crack. Data should be reported for the same load points reported in Question 1 for the best estimate of the load–displacement curve. Results should be reported with at least the same level of resolution in the force/displacement increments and areal resolution based on force–displacement data that corresponds to a DIC image. Report all values relative to the undeformed original state coordinate system.

- All challengers reported results for this question. However, the corresponding experimental results were not derived (only a final experimental crack geometry) at the time of this publication. In addition, the simulation results reported for this question were not

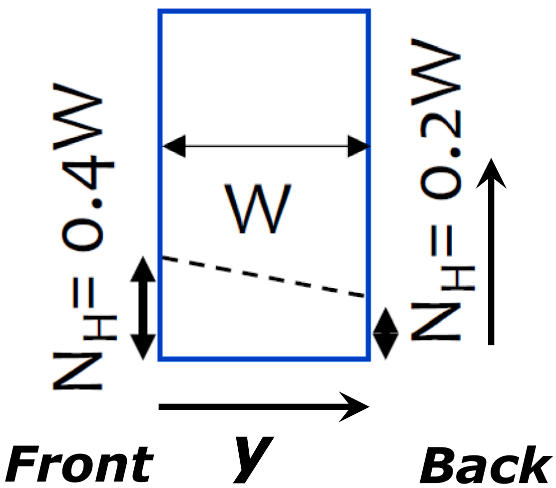

Fig. 8. The challenge geometry included an offset angled, non-uniform depth notch, intended to induce I, II, and III modes of failure.

necessarily of sufficient density in space, on account of the simulated crack tip only being reported at specific moments in time corresponding to discrete loading states. Consequently, it was not possible to perform a direct comparison between the time dependent predicted and load-dependent crack evolution, nor use the answers to this question to meaningfully compare against the final observed crack state.

Challenge Question 3: Report the displacements (D_x, D_y & D_z in millimeters – change in position relative to the undeformed state) of the front and back faces of the sample for the entire loading cycle for the same load points as in Question 1 from initial loading through post-peak failure. Report values relative to the undeformed state coordinate system. Report initial undeformed position of the points (add extra files).

- All challengers reported results for this question. Similarly, digital image correlation (DIC) displacement fields were obtained during the experiment. However, differences between the numerical and experimental acquisitions made quantified comparison problematic. In particular, the experimental result exhibited more rigid-body motions of the two pieces than was observed with the simulations. In addition, detailed quantitative comparison of the displacement fields can only be made for cracks with identical geometry. Finally, the timing of the crack propagation was different for each participant, further complicating a direct comparison.

Discussion Question 1: Report variability of your model based on the laboratory calibration data ––does the model have any inherent variability?

- None of the modelers appeared to include variability, or stochastic treatments, within their simulations. In addition, none of the models directly accounted for roughness of the fracture surfaces.

Bonus Science Question: Report the *x*, *y*, and *z* coordinates of the two fracture surfaces (in millimeters) at the end (final load) of the simulation based on the best estimate simulation reported for Question 1. If there is more than 1 crack, report for all.

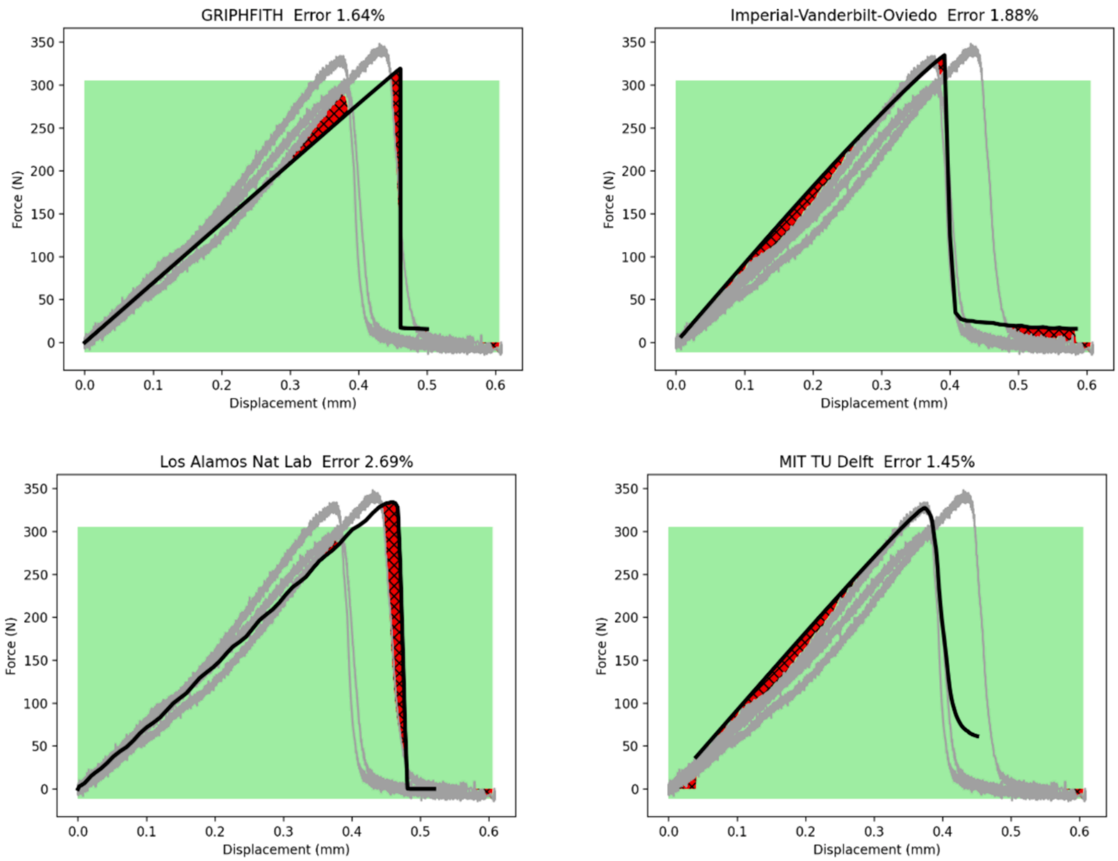

Fig. 9. The force–displacement predictions from all teams that participated in the challenge phase. We observe that all were able to match the envelope of the experimental force–displacement data to within a couple of percent.

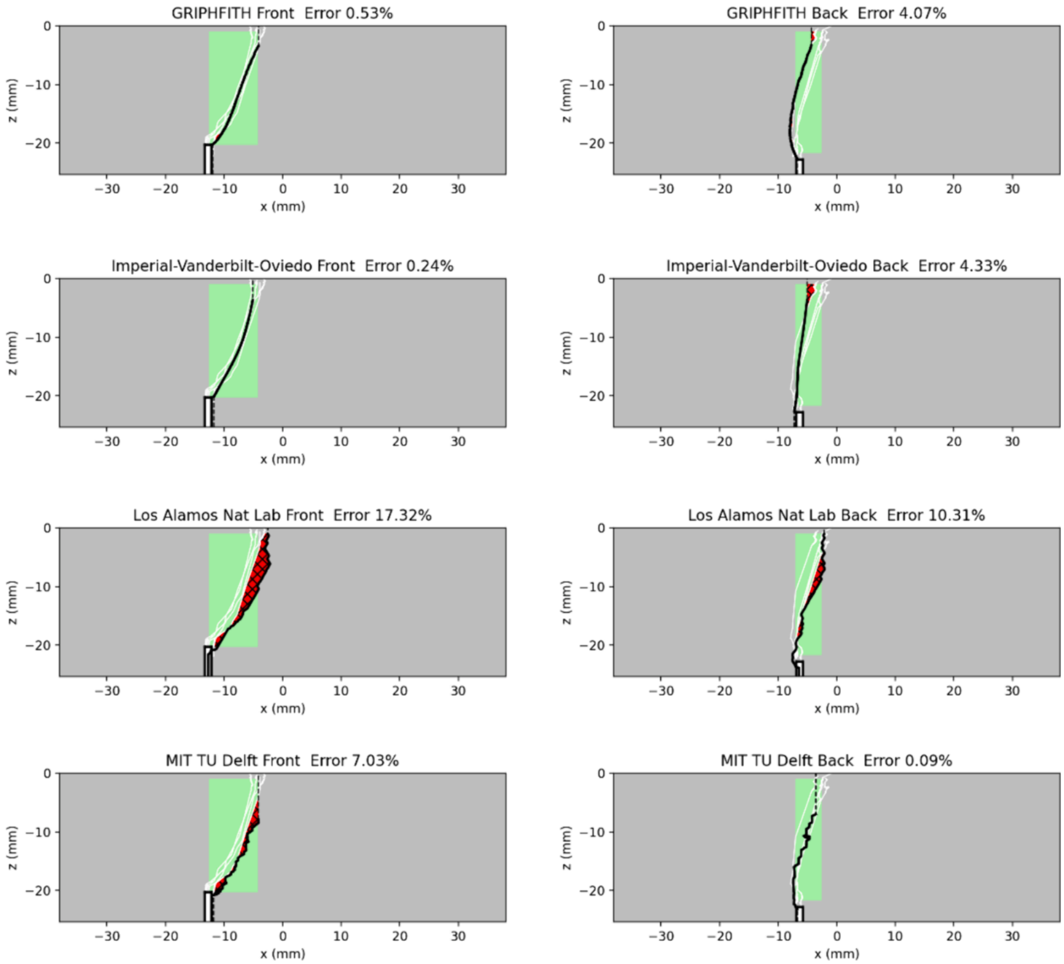

Fig. 10. Comparison of participants challenge submissions for crack geometry (black lines, with dashes indicating extrapolation to the edge of the test article) compared with the data (white lines). Generally, crack geometry was well predicted, with some participants doing a better job of capturing the curvature of the crack on the front and back face. The initial notch is shown in white, with black outline. Discrepancies between prediction and observation are highlighted in red with black cross-hatching. The green rectangle is the reference area used to normalize the error calculation.

- All challengers reported answers to this question. At the time of the intercomparison, the full post-processing of the experiment had not been completed and only the final crack geometry from images of the front and back of the test article were available. The answers to this question were used to obtain simulated trajectories of the cracks on the front and back of the test article for comparison with observation.

The blind predictions of the load displacement response are shown in Fig. 9 and the final crack geometries submitted are shown in Fig. 10 and Fig. 11. In general, all participants achieved good agreement with observations. The force–displacement response was consistent among the teams with some differences in the surface expression of the crack. The calibration phase clearly enabled teams to focus on which elements of the calibration data set were of most predictive value. However, it is worth noting that although challengers were able to predict the force–displacement response within the envelope of experimental results, none of them captured the stiffening observed in all of the experimental results. Simulated force–displacement curves (Fig. 9) are essentially linear up to peak loading, while each experimental curve is concave up. In addition, the post-peak behavior for the majority of teams was very sudden. The exception is MIT TU Delft, whose post-failure response exhibits residual strength softening behavior that qualitatively resembles observations (Fig. 9). Table 2 provides an overall summary of the quantified error metrics and other observations for each of the participants.

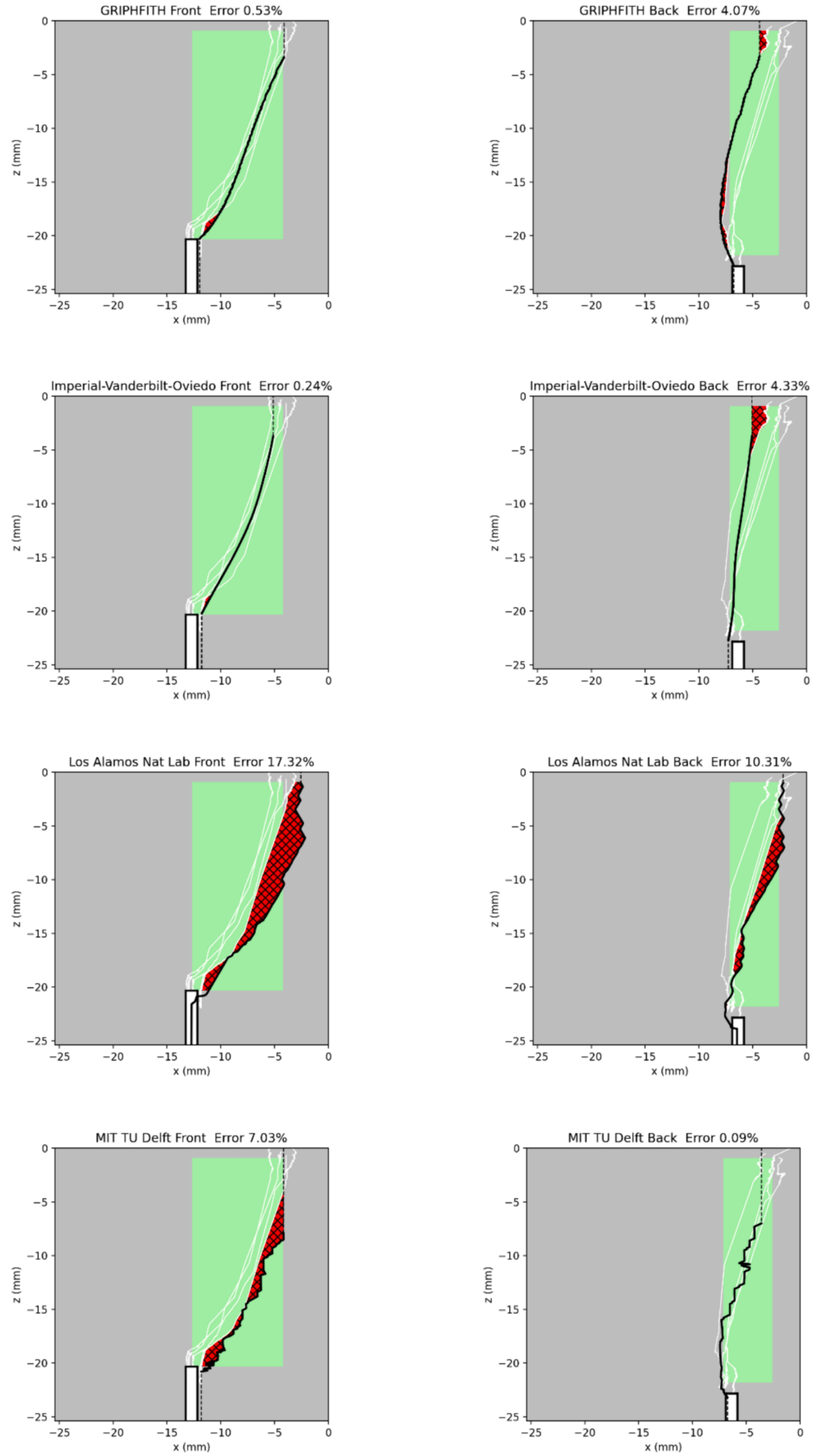

Fig. 11. Zoomed-in comparison of participants challenge submissions for crack geometry (black lines, with dashes indicating extrapolation to the edge of the test article) compared with the data (white lines). Generally, crack geometry was well predicted, with some participants doing a better job of capturing the curvature of the crack on the front and back face. The initial notch is shown in white, with black outline. Discrepancies between prediction and observation are highlighted in red with black cross-hatching. The green rectangle is the reference area used to normalize the error calculation.

7. Discussion

The biggest hurdle to the competitors was identifying which calibration data was of most utility. Conducting information exchange during the calibration phase helped ensure that all participants were making full and optimal use of the calibration data. Having completed calibration, it was apparent that the force–displacement response of the challenge geometry was apparently easy to predict (all competitors' predictions were within a couple of percent). It is possible that the calibration data may have been too comprehensive to make the force–displacement challenge prediction truly challenging. In contrast, the crack trajectories were predicted with less accuracy (5% to 20% error) and also did not always show the same curvature of the cracks. This was most clearly the case for finite element solutions where the mesh was guiding the orientation of the cracks. This would indicate that matching force–displacement response during material failure may not be indicative of a model correctly capturing the internal mode of failure of the object. Consequently, a model demonstrating good performance for one set of loading conditions may not retain predictive power for different loading conditions.

The phase field methods generally showed the lowest error for the crack geometry. The finite element methods (whether traditional finite element or discontinuous Galerkin) showed evidence of mesh effects that caused the crack propagation to deviate from the experimentally observed path. That said, finite element methods are generally simpler algorithmically and have mature approaches for either iteratively or implicitly coupling to other processes, such as fluid-driven fracture, to enable multiphysics solutions. In addition, it may have been possible to improve the performance of these methods by intentionally randomizing the mesh geometry (see Sherman [15,16]). Incorporation of multiple, coupled physical processes is still an area of active research for phase field methods. In addition, phase field methods are more computationally expensive for comparable resolution.

Unfortunately, PFC methods were only used during the calibration phase and results were not provided for the challenge problem. As mentioned earlier, a perceived disadvantage of PFC methods is that the bond constitutive law generally needs to be calibrated to mechanical response. However, we observed that all participants necessarily had to calibrate their models against the response of the notched specimens because they used models that assumed a constant elastic modulus (independent of load) and the ultrasonic measurements corresponded to a higher stiffness than that exhibited by the samples during 3-point bending. We conclude that the models should be using a nonlinear stiffness that reproduces the change in stiffness with strain, rather than fit the elastic properties for a single, representative loading condition. Wang et al [17] used PFC to simulate fracture surface roughness observed for 3D printed gypsum samples subjected to 3-point bending. They noted that to match the variations in surface roughness and peak load values required inclusion of the structure and mineral fabric orientation in the simulations. Peak load was affected by the strength of the mineral/bonds directly over the notch.

8. Conclusions

We conclude that multiple numerical methods can be calibrated to predict the brittle-ductile failure of 3D printed rock-surrogate materials. The Damage Mechanics Challenge was successful in many of the original objectives:

1. Compare computational approaches for damage evolution for predicting fracture behavior of 3D printed model rock:
   - o Between the Calibration and Challenge phases, four different classes of methods were applied (Finite/Discrete Element Method, Phase Field, Hybrid Discontinuous Galerkin, Particle Flow Code). All four were able to be calibrated to fit observations during the Calibration phase. However, only FDEM and Phase Field were exercised for the Challenge phase.
2. Identify the information provided by the different simulation approaches that gives insight into the prediction and interpretation of failure in rock:
   - o Matching ultrasonic data alone for elastic properties led to an overly stiff mechanical response.
   - o The best calibrations and predictions were obtained by focusing on matching the 3-point bending tests; however, it was possible to match the force–displacement response for the 3-point bending tests and yet not reproduce the crack geometry well.
3. Identify model parameters that are currently not measured or cannot be measured in the laboratory:
   - o All of the numerical methods had various parameters that are not directly measured (for example, the intrinsic length scale used in phase field methods); however, the macroscopic response of the large number of 3-point bending tests was sufficient to calibrate these parameters.
4. Determine whether there are other experimental measurements that are needed or better methods of performing measurements to monitor damage evolution:
   - o Ultimately, this aspect of the Challenge was not completely addressed. Although participants were able to match force–displacement and crack trajectory using the calibration data, there were attributes of the simulation results that were not reported where major discrepancies could remain. Specifically, none of the participants provided data on crack roughness or uncertainty, both of which are quantities of relevance to real-world system performance.
   - o In terms of monitoring of damage evolution, it was clear that matching the force–displacement response did not ensure an accurate crack geometry. This has implications for in situ monitoring of structural failure, where it is possible that a model may match external stress–strain observables and fail to predict the details of the failure mode.

In addition to the above, we were able to identify several lessons learned pertaining both to the execution of Challenges in general and monitoring/prediction of brittle-ductile failure:

Table 2
Error estimations for the challenge predictions and general performance observations. A perfect score corresponds to 0% and 0 mm shift.

Team	Force-disp. %	Area-based error Front %	Back %	Linear-based error Front %, shift [mm]	Back %, shift [mm]	Observations
GRIPHFITH (Phase Field)	1.6	0.5	4.1	19.2, −0.5	12.1, 0.5	Loading slightly less-stiff than experiment, unloading goes to zero instantly, excellent crack shape, but does not propagate to edge
Imperial-Vanderbilt-Oviedo (Phase Field)	1.9	0.2	4.3	15.2, −0.5	27.3, −0.1	Loading slightly stiffer than experiment, unloading has slope similar to one of experiments, simulation terminates with residual force, excellent crack shape, but does not propagate to edge
LANL (FDEM)	2.7	17.3	10.3	24.2, −2.4	20.2, −1.4	Loading fits envelop of data but does not stiffen, unloading exhibits some slope, but steeper than experiment, achieves zero final force, crack trajectory shows mesh imprinting and deviates, crack extends to edge.
MIT TU Delft (Hybrid Discontinuous Galerkin)	1.5	7.0	0.09	38, 1.6	34.3, 0.1	Loading does not start from zero, slope steeper than experiment, unloading slope is within experiments, does not return to zero force, crack geometry exhibits mesh imprinting and does not propagate to the edge.

- For the application of any method to be successful, the calibration data must be relevant to the scenario of interest. Our observation during the challenge was that the teams were able to learn from the calibration phase to focus upon calibration data of most relevance to the question being asked for the challenge problem. Specifically, ultrasonic data implied a higher stiffness than that exhibited by the test materials during 3-point bending tests.
- The relative ease with which participants matched the challenge geometry suggests that the calibration data were too similar to the challenge problem or too comprehensive. A better challenge would involve a geometry that is significantly different from the calibration dataset.
- Phase Field models provided the most realistic crack path geometry in this challenge, while the FDEM and Discontinuous Galerkin methods both exhibited mesh imprinting that led to larger errors in crack geometry. Additionally, at this point in method maturity, FDEM and DG methods have well-established approaches to coupled multiphysics that remain an area of research for Phase Field approaches. Furthermore, mesh sensitivity with FDEM and DG methods can be mitigated to some extent with intentionally randomized meshes.
- Finally, the methods for comparing simulation with experiment are open to refinement. From the outset of the Challenge, the agreed approach for this challenge was to compare simulations to the envelope of the experimental results. This approach was intended to avoid penalizing modelers for variability in the experimental results. However, a consequence was that numerical predictions that qualitatively differ in character from observations may still fit within the envelope and have zero error. There were examples where the curvature of either force–displacement results or crack trajectories differed from experiment but remained within the spread of observations. Methods of comparison that re-baseline results into a common coordinate system (e.g., via affine transformation) where comparisons can be made may be helpful here.

LJPN, AB and LJ acknowledge support of the experimental work and data curation by the National Science Foundation CMMI 1932312. HY was supported by the Laboratory Directed Research and Development program (218328) at Sandia National Laboratories. This work was performed under the auspices of the U.S. Department of Energy by Lawrence Livermore National Laboratory under Contract DE-AC52-07NA27344. Sandia National Laboratories is a multi-mission laboratory managed and operated by National Technology & Engineering Solutions of Sandia, LLC (NTESS), a wholly owned subsidiary of Honeywell International Inc., for the U.S. Department of Energs National Nuclear Security Administration (DOE/NNSA) under contract DE-NA0003525.written work is authored by an employee of NTESS. The employee, not NTESS, owns the right, title and interest in and to the written work and is responsible for its contents. The publisher acknowledges that the U.S. Government retains a non-exclusive, paid-up, irrevocable, world-wide license to publish or reproduce the published form of this written work or allow others to do so, for U.S. Government purposes. The DOE will provide public access to results of federally sponsored research in accordance with the DOE Public Access Plan. This paper describes objective technical results and analysis. Any subjective views or opinions that might be expressed in the paper do not necessarily represent the views of the U.S. Department of Energy or the United States Government.

CRediT authorship contribution statement

J.P. Morris: Writing – review & editing, Writing – original draft, Visualization, Project administration, Methodology, Investigation, Formal analysis, Conceptualization. **L.J. Pyrak-Nolte:** Writing – review & editing, Project administration, Methodology, Investigation, Formal analysis, Data curation, Conceptualization. **H. Yoon:** Writing – review & editing, Methodology, Investigation, Formal analysis, Data curation, Conceptualization. **A. Bobet:** Writing – review & editing, Methodology, Investigation, Formal analysis, Conceptualization. **L. Jiang:** Writing – review & editing, Validation, Methodology, Investigation, Formal analysis, Data curation.

Declaration of competing interest

The authors declare that they have no known competing financial interests or personal relationships that could have appeared to influence the work reported in this paper.

Data availability

The data associated with the Damage Mechanics Challenge is available from: https://purr.purdue.edu/groups/damagemechanicschallenge and the derived data (e.g., error analysis) presented for the intercomparison here will be made available on request.

Acknowledgment

LJ is currently supported by the Shuimu Tsinghua Scholar Program from Tsinghua University, China.

References

[1] Bobet A, Fakhimi A, Johnson S, Morris J, Tonon F, Yeung M. Numerical Models in Discontinuous Media: Review of Advances for Rock Mechanics Applications. J Geotech Geoenviron Engng 2009;135(11):2009. https://doi.org/10.1061/(ASCE)GT.1943-5606.0000133.
[2] Boyce BL, et al. The Sandia Fracture Challenge: blind round robin predictions of ductile tearing. Int J Fract 2014;186:5–68.
[3] Block G, Rubin MB, Morris J, Berryman JG. Simulations of dynamic crack propagation in brittle materials using nodal cohesive forces and continuum damage mechanics in the distinct element code LDEC. Int J Fract 2007;2007(144):131–47. https://doi.org/10.1007/s10704-007-9085-2.
[4] Heister T, Wheeler MF, Wick T. A primal-dual active set method and predictor-corrector mesh adaptivity for computing fracture propagation using a phase-field approach. Comput Methods Appl Mech Eng 2015;290:466–95.
[5] Jenabidehkordi A. Computational methods for fracture in rock: a review and recent advances. Front Struct Civ Eng 2019;13:273–87. https://doi.org/10.1007/s11709-018-0459-5.
[6] Jiang L, Yoon H, Bobet A, Pyrak-Nolte LJ. Mineral fabric as a hidden variable in fracture formation. Sci Rep 2020;10, Article number 2260. https://doi.org/10.1038/s41598-020-58793-y.
[7] Jiang L, Yoon H, Pyrak-Nolte LJ, Bobet A, Morris J. Calibration Data Set for Damage Mechanics Challenge on Brittle-Ductile Material. Purdue University Research Repository 2021. https://doi.org/10.4231/QF39-Q924.
[8] Jiang L, Pyrak-Nolte L, Yoon H, Bobet A, Morris J. Digital Image Correlation data, X-ray CT, XRD and Ultrasonic Data Sets for Damage Mechanics Challenge on Brittle-Ductile Material. Purdue University Research Repository 2021. https://doi.org/10.4231/2E8M-W085.
[9] Jing L, Hudson J. Numerical methods in rock mechanics. Int J Rock Mech Min Sci 2002;39(4):409–27.
[10] Morris JP, Rubin MB, Block GI, Bonner MP. Simulations of fracture and fragmentation of geologic materials using combined FEM/DEM Analysis. J Impact Eng 2006;33:463.
[11] O'brien JF, Hodgins JK. Graphical modeling and animation of brittle fracture. In the proceedings of ACM SIGGRAPH 99, Computer Graphics Proceedings, Annual Conference Series, 137–146. 1, 2; 1999.
[12] Ortiz M, Pandolfi A. Finite-deformation irreversible cohesive elements for three-dimensional crack-propagation analysis. Int J Numer Meth Eng 1999;44:1267–82.
[13] Radovitzky R, Seagraves A, Tupek M, Noels L. A scalable 3D fracture and fragmentation algorithm based on a hybrid, discontinuous Galerkin, Cohesive Element Method. Comput Methods Appl Mech Engng 2011;200:326–44. https://doi.org/10.1016/j.cma.2010.08.014.
[14] Settgast RR, Fu P, Walsh SDC, White JA, Annavarapu C, Ryerson FJ. A fully coupled method for massively parallel simulation of hydraulically driven fractures in 3-dimensions. Int J Numer Anal Meth Geomech 2017;41:627–53.
[15] Sherman, C., Morris, J., Johnson, S., Savitski, A. (2015a). Modeling of Near-Wellbore Hydraulic Fracture Complexity. 10.15530/urtec-2015-2153274.
[16] Sherman, C. S., Aarons, L. R., Morris, J. P., Johnson, S., Savitski, A. A., and Geilikman, M. B. (2015b). Finite element modeling of curving hydraulic fractures and near-wellbore hydraulic fracture complexity. In *Proceedings of the 49th US Rock Mechanics/Geomechanics Symposium*. American Rock Mechanics Association.
[17] Wang C, Jiang L, Bobet A, Yoon H, Pyrak-Nolte LJ. Fabric controls on fracture surface roughness of an architected rock material. Mech Res Commun 2024;135:104223.
[18] Zhuang X, Zhou S, Huynh GD, Areias P, Rabczuk T. (2022) Phase field modeling and computer implementation: A review. Engng Fract Mech 2022;262:108234.
[19] Navidtehrani Y, Duddu R, Martínez-Pañeda E. Damage Mechanics Challenge: Predictions based on the phase field fracture model. Eng Fract Mech 2024;301:110046. https://doi.org/10.1016/j.engfracmech.2024.110046. ISSN 0013-7944.
[20] Pickard D, Quinn C, Giovanardi B, Radovitzky R. Blind prediction of curved fracture surfaces in gypsum samples under three-point bending using the Discontinuous Galerkin Cohesive Zone method. Eng Fract Mech 2024;306:110205. https://doi.org/10.1016/j.engfracmech.2024.110205. ISSN 0013-7944.
[21] Gupta A, Nguyen DT, Hirshikesh, Duddu R. Damage mechanics challenge: Predictions from an adaptive finite element implementation of the stress-based phase-field fracture model. Eng Fract Mech 2024;306:110252. https://doi.org/10.1016/j.engfracmech.2024.110252. ISSN 0013-7944.
[22] Heinzmann J, Carrara P, Luo C, Manav M, Mishra A, Nagaraja S, Oudich H, Vicentini F, De Lorenzis L. Calibration and validation of a phase-field model of brittle fracture within the damage mechanics challenge. Eng Fract Mech 2024;307:110319. https://doi.org/10.1016/j.engfracmech.2024.110319. ISSN 0013-7944.
[23] Euser B, Padilla A, Lei Z, Knight E, Munjiza A, Rougier E. Blind prediction of fracture in an additively manufactured geomaterial using the finite discrete element method. Eng Fract Mech 2024;307:110257. https://doi.org/10.1016/j.engfracmech.2024.110257. ISSN 0013-7944.